Chaos and damping in the post-Newtonian description of spinning compact binaries

Neil J. Cornish
Department of Physics, Montana State University, Bozeman, Montana 59717, USA

Janna Levin
DAMTP, Cambridge University, Wilberforce Road, Cambridge CB3 0WA, United Kingdom

(Received 2 July 2002; published 1 July 2003)

Binary systems of rapidly spinning compact objects, such as black holes or neutron stars, are prime targets for gravitational wave astronomers. The dynamics of these systems can be very complicated due to spin-orbit and spin-spin couplings. Contradictory results have been presented as to the nature of the dynamics. Here we confirm that the dynamics—as described by the second post-Newtonian approximation to general relativity—is formally chaotic, despite claims to the contrary. When dissipation due to higher order radiation reaction terms is included, the chaos is damped. The damping time scale is found to be comparable to, but shorter than, the time scale that characterizes the chaotic behavior. This result suggests that the gravitational waveforms computed to 2.5 post-Newtonian order from spinning compact binaries will not suffer from sensitive dependence on initial conditions. If the post-Newtonian approximation at this order is an adequate description, then the waves can be detected using standard hierarchical matched filtering techniques. On the other hand, the competition between chaotic decoherence and radiation induced dissipation is close enough that the merger history does retain an imprint of the chaotic behavior. Moreover, the time scales are sufficiently close, and the post-Newtonian approximation is sufficiently crude, that we cannot rule out the possibility that chaotic effects play a role in real binary systems.

DOI: 10.1103/PhysRevD.68.024004 PACS number(s): 04.30.Db, 04.25.Nx, 05.45.Jn, 95.30.Sf

Gravitational wave astronomy blurs the lines between theory and observation by requiring accurate source modeling to facilitate detection. While it is possible to detect gravitational waves without precise waveform templates, matched filtering against a template bank is the only way to extract detailed information about the sources. A template based, matched filtering approach to gravitational wave data analysis is impractical if the orbital dynamics is chaotic [1–4]. Systems that exhibit sensitive dependence to initial conditions require template banks that are exponentially larger than those of nonchaotic systems.

Spinning compact binaries pose a challenge to template based detection and parameter extraction techniques. The waveforms depend on a large number of parameters, including the masses of the two bodies, their spins, and the relative alignment of the spin and orbital angular momentum—some 11 parameters in all. Even with a relatively coarse sampling of parameter space, the resulting template bank can be very large. The hope is that hierarchical schemes can be used that start with a coarse sampling and proceed by successive refinement [5]. However, template based methods, hierarchical or otherwise, will not work if the underlying dynamics is chaotic. The sensitivity to initial conditions that characterizes chaotic systems implies that waveforms that are initially nearby (as measured by their cross correlation over some time interval) will diverge exponentially with time [3].

A debate has arisen as to whether spinning compact binaries exhibit chaotic behavior. The first indication of chaotic behavior was found using a test particle approximation [1], but chaotic orbits were only found for unphysically large values of the particle's spin. The problem was also approached using the post-Newtonian approximation to general relativity, and fractal methods were used to show that binaries with realistic spins exhibited chaotic behavior at second post-Newtonian (2PN) order [2]. Commentaries were written emphasizing that radiation reaction would damp the chaos [6], and that the post-Newtonian approximation was being pushed beyond its domain of validity [7], although unavoidably since no better approximation is available. However, neither commentary disputed the central result of Refs. [2,4]—that the second post-Newtonian equations of motion admit chaotic behavior. Then a paper was published ''ruling out chaos in compact binary systems'' [8]. This study used the same 2PN equations of motion, but a different method for establishing chaos—Lyapunov exponents rather than fractals. The results reported in Refs. [2] and [8] sit in stark contrast. The trajectories that form the fractal basin boundaries found in [2] belong to a set of unstable periodic orbits known as the strange repellor. These orbits must have positive Lyapunov exponents. Trajectories near the boundaries will also have positive Lyapunov exponents, as may orbits that lie far from the boundaries.

In what follows, we refute the claims made in Ref. [8] by showing that the 2PN equations of motion do admit orbits with positive Lyapunov exponents.

After establishing the presence of chaos, we then explore the significance of this result by comparing three key time scales in the problem—the average orbital period T_o, the Lyapunov time T_λ, and the decay time T_d. If T_λ is short compared to T_d, the chaotic dynamics seen in the conservative 2PN system will leave a strong imprint on the 2.5PN dissipative dynamics. On the other hand, if the Lyapunov time is long compared to the decay time, there will not be a chance for the orbits to diverge before the plunge and matched filtering will not be substantially degraded.

For the specific binary orbits studied we find that $T_\lambda \gtrsim 2T_d$. This tells us that the damping due to gravitational wave emission is stronger than the instability seen in the undamped dynamics. In other words, the gravitational waveforms predicted by the 2.5PN dynamics will not suffer from sensitive dependence on initial conditions, so these waves could be detected using a template based, matched filtering approach. We have to be a little cautious about using this result to draw conclusions about real astrophysical systems. The chaotic effects seen at 2PN order become more pronounced as the spins or velocities are increased, which pushes the system into a realm where the post-Newtonian approximation starts to break down. While we expect the post-Newtonian approximation to provide a fair qualitative description of the dynamics, it may be unwise to place too much faith in the quantitative relationship between T_λ and T_d.

The post-Newtonian equations of motion are written as a series expansion in v^2/c^2, where v is the relative velocity and c is the speed of light:

$$\mu\ddot{\mathbf{r}} = \mathbf{F}_N^{(0)} + \mathbf{F}_{PN}^{(1)} + \mathbf{F}_{SO}^{(1.5)} + \mathbf{F}_{PN}^{(2)} + \mathbf{F}_{SS}^{(2)} + \mathbf{F}_{QM}^{(2)} + \mathbf{F}_{RR}^{(2.5)} + \mathbf{F}_{SO}^{(2.5)} + \mathbf{F}_{PN}^{(3)} + \mathbf{F}_{SS}^{(3)} + \ldots . \quad (1)$$

Here $\mu = m_1 m_2 / M$ is the reduced mass, $M = m_1 + m_2$ is the total mass, and $\ddot{\mathbf{r}}$ is the relative acceleration of the two bodies. In these units $G = c = 1$ so that all lengths are measured in units of the total mass M. The product $\mu\ddot{\mathbf{r}}$ is given in terms of a series of forces, starting with the usual Newtonian force $\mathbf{F}_N^{(0)} = m_1 m_2 \mathbf{r}/r^3$. The superscripts denote the order of the post-Newtonian expansion and the subscripts denote the type of force. The explicit form of the higher order terms can be found in Refs. [9–11]. Qualitatively, the 1PN force $\mathbf{F}_{PN}^{(1)}$ introduces perihelion precession. The 2PN force $\mathbf{F}_{PN}^{(2)}$ introduces isolated unstable orbits, along with an innermost stable circular orbit (ISCO), and the possibility of merger. The 1.5PN spin-orbit force $\mathbf{F}_{SO}^{(1.5)}$ leads to precession of the orbital plane, as do the 2PN spin-spin $\mathbf{F}_{SS}^{(2)}$ and spin-induced quadrupole-monopole $\mathbf{F}_{QM}^{(2)}$ forces. The spin-spin force is attractive for spins that are aligned and repulsive for spins that are antialigned. The 2.5PN order radiation reaction force, $\mathbf{F}_{RR}^{(2.5)}$, is the first nonconservative term, and it causes the orbital energy E and angular momentum $\mathbf{L}$ to decay. Associated with the spin-orbit and spin-spin forces are torques that act on the spin of each body, causing the spins to precess—see Ref. [9] for details. To date, the expansion is known up to 3PN order only under the very restrictive conditions of no spins and/or circular or quasicircular orbits. In order to explore the range of all orbits, including noncircular orbits with spins, we consider terms up to 2.5PN order as was done in Refs. [2,8]. We also neglect the 2PN quadrupole-monopole and 2.5PN spin-orbit forces. The PN approximation in general has many shortcomings. The convergence of the expansion to the full relativistic problem is very slow and therefore does not reflect the full nonlinearity of the relativistic two-body system. Additionally, for the innermost orbits, the expansion parameter v^2/c^2 is getting big enough to challenge the validity of the approximation. Nonetheless, the PN approximation is the only description currently available. If any alternative descriptions do become available, they too can be tested for the presence of chaos. In further defense of these approximations, we point out that the terms that we keep capture the main *qualitative* features expected from full general relativity. If anything, the higher order nondissipative terms are likely to increase the strength of the chaotic behavior.

The dynamics takes place in a 12-dimensional phase space with coordinates $\vec{X} = (\mathbf{x}, \mathbf{p}_x, \mathbf{S}_1, \mathbf{S}_2)$, where $\mathbf{p}_x$ is the momentum conjugate to $\mathbf{x}$, and $\mathbf{S}_i$ describes the spins of the two bodies. In the absence of radiation reaction there are 6 conserved quantities, the energy E, total angular momentum $\mathbf{J} = \mathbf{L} + \mathbf{S}_1 + \mathbf{S}_2$ and spin magnitudes $|\mathbf{S}_i|$. Linearizing the equations of motion about a reference trajectory $\vec{X}(t)$ gives the evolution of the difference $\delta\vec{X}(t)$

$$\delta\dot{X}_i(t) = \left.\frac{\partial \dot{X}_i}{\partial X_j}\right|_{\vec{X}(t)} \delta X_j(t) \equiv K_{ij}(t)\,\delta X_j(t). \quad (2)$$

The solution to this equation can be written:

$$\delta X_i(t) = L_{ij}(t)\,\delta X_j(0). \quad (3)$$

The evolution matrix $L_{ij}(t)$ is given in terms of the linear stability matrix K_{ij} by

$$\dot{L}_{ij} = K_{il} L_{lj}, \quad (4)$$

with $L_{ij}(0) = \delta_{ij}$ (repeated indices imply summation). The Lyapunov exponents are defined [12] in terms of the eigenvalues $\Lambda_i(t)$ of the distortion matrix $\Lambda_{ij} = L_{il} L_{lj}$:

$$\lambda_i = \lim_{t\to\infty} \frac{1}{2t} \log \Lambda_i(t). \quad (5)$$

The 2PN equations of motion are conservative and can be derived from a Hamiltonian. The expansion and vorticity of the flow vanishes for Hamiltonian systems (in canonical coordinates), so that $\det(\Lambda_{ij}) = 1$, $\Lambda_{ij} = \Lambda_{ji}$ and the Lyapunov exponents come in $+/-$ pairs that measure the exponential shearing of the flow. The principal Lyapunov exponent $\lambda_p = \max(\lambda_i)$ can be calculated without directly isolating the eigenvalues from

$$\lambda_p = \lim_{t\to\infty} \frac{1}{2t} \log\left(\frac{\Lambda_{jj}(t)}{\Lambda_{jj}(0)}\right). \quad (6)$$

In the limit of very long times, the principal positive Lyapunov exponent will dominate the trace in Eq. (6).

By contrast, the quantity calculated in Ref. [8] was

$$\lambda_d = \lim_{t\to\infty} \lim_{dX(0)\to 0} \frac{1}{t} \log\left(\frac{dX(t)}{dX(0)}\right) \quad (7)$$

with $dX = \{[X_i(t) - Y_i(t)][X_i(t) - Y_i(t)]\}^{1/2}$ the Cartesian distance between the 12-component vectors of a reference

trajectory $\vec{X}(t)$ and a nearby shadow trajectory $\vec{Y}(t)$. It must be emphasized that this is *not* a Lyapunov exponent. Equation (7) will automatically yield zero for bound orbits when the limit $t\to\infty$ is taken as $dX(t)$ must remain finite. Equation (7) can represent an *approximation* to the Lyapunov exponent if an additional rescaling of the shadow trajectories is incorporated. The rescaling is accomplished by determining when $dX(t_r)>RdX(0)$ for some threshold R, then starting a new shadow trajectory $\vec{Y}'(t)$ with initial conditions

$$\vec{Y}'(t_r)=\vec{X}(t_r)+[\vec{Y}(t_r)-\vec{X}(t_r)]/R. \tag{8}$$

The rescaling is repeated throughout the evolution to ensure that one is accurately approximating the stability of the reference trajectory $X(t)$. The problem with this method is that the choice of threshold can significantly affect the value of λ_d. This may explain the disagreement between our results and those in Ref. [8]. A far more robust method is to evolve the perturbation $\delta\vec{X}(t)$ directly using Eq. (2). No rescaling is needed as Eq. (2) defines the dynamic stability without approximation.

A second more subtle point to make regarding Eq. (7) is that while $dX(t)$ is often referred to as the ''distance between nearby trajectories in phase space,'' this statement is misleading as phase space does not admit a metric structure. Even if rescaled properly so that $dX(t)\approx\delta X(t)$ from Eq. (2), the distance $dX(t)$ only measures the projection of the distortion matrix onto the initial displacement vector:

$$d^2X(t)\approx d^2(t)=dX_i(0)\Lambda_{ij}(t)dX_j(0). \tag{9}$$

As a consequence of this additional approximation, λ_d provides only a lower bound for λ_p.

We use three methods to estimate the principal Lyapunov exponent:

Method (A) determines the full evolution matrix L_{ij} from Eq. (4) and uses Eq. (6) to calculate λ_p. This is the most numerically intensive method as it involves integration of the 144 components of the evolution matrix L_{ij} as well as the 12 components of the trajectory itself. The advantage of this method is that it yields an unambiguous computation of the stability of an orbit with no approximations.

Method (B) uses shadow trajectories and Eq. (7) with a careful rescaling of the shadow orbit. This method involves the approximation of Eq. (7), along with rescaling and the projection described by Eq. (9).

Method (C) uses Eq. (2) to evolve $\delta\vec{X}(t)$ along the reference trajectory $\vec{X}(t)$ so that a total of 24 equations are integrated and used to calculate

$$\lambda_c=\lim_{t\to\infty}\lim_{\delta X(0)\to 0}\frac{1}{t}\log\left(\frac{\delta X(t)}{\delta X(0)}\right). \tag{10}$$

This method combines the accuracy of integrating the stability equations with the approximation of projecting onto the distortion matrix as in Eq. (9).

In addition to these methods we also studied the rate of phase decoherence in the waveforms of the reference and shadow trajectories. According to Ref. [3], the phase difference $|\delta\Phi(t)|$ should grow as $e^{\lambda_p t}$. In summary, all four methods for estimating λ_p use some measure $D(t)$, where $D(t)$ is equal to $\Lambda_{jj}^{1/2}(t)$, $dX(t)$, $d(t)$ or $|\delta\Phi(t)|$, depending on the method. In each case, the quantity $D(t)$ will have an initial power-law rise that is followed by exponential growth for unstable orbits.

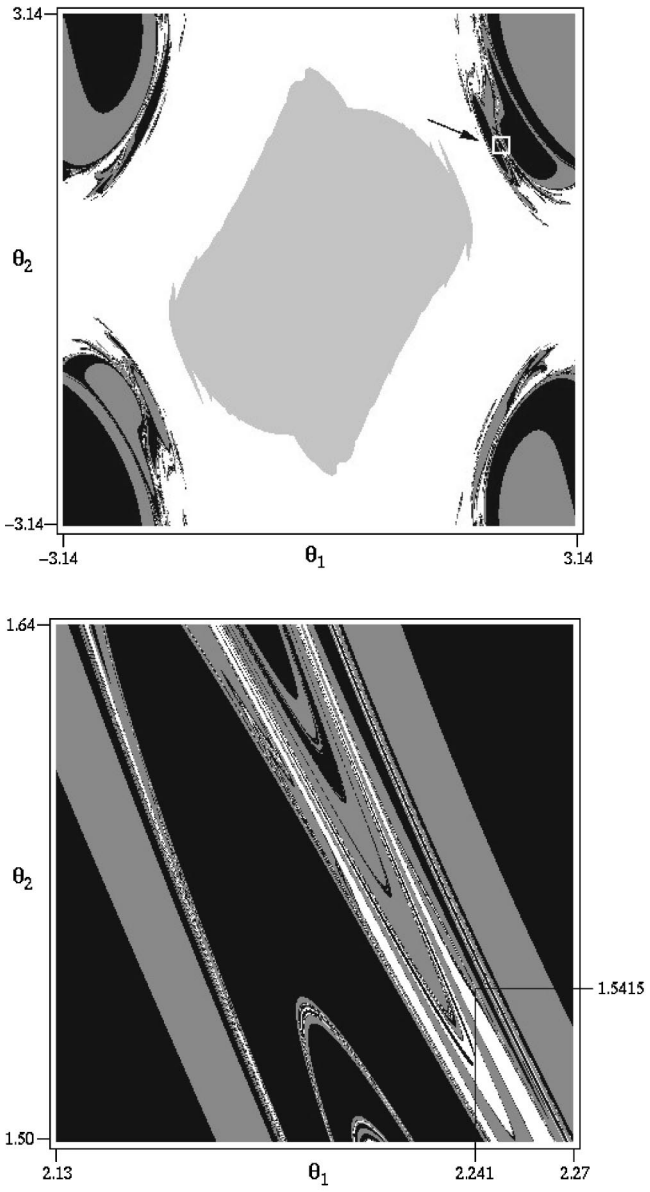

FIG. 1. Fractal basin boundaries showing three possible outcomes for the binary system as a function of the initial spin alignments.

The equations of motion and the linearized evolution matrix $L_{ij}(t)$ were evolved using a fourth order Runge-Kutta integrator with adaptive step size. The six quantities, E, $\mathbf{J}$, $|\mathbf{S}_1|$ and $|\mathbf{S}_2|$ were monitored to ensure that they were conserved at 2PN order.

To illustrate the connection between the fractal structures and Lyapunov exponents, we begin by regenerating Fig. 3 of Ref. [2] in our Fig. 1. The trajectories were started in the x

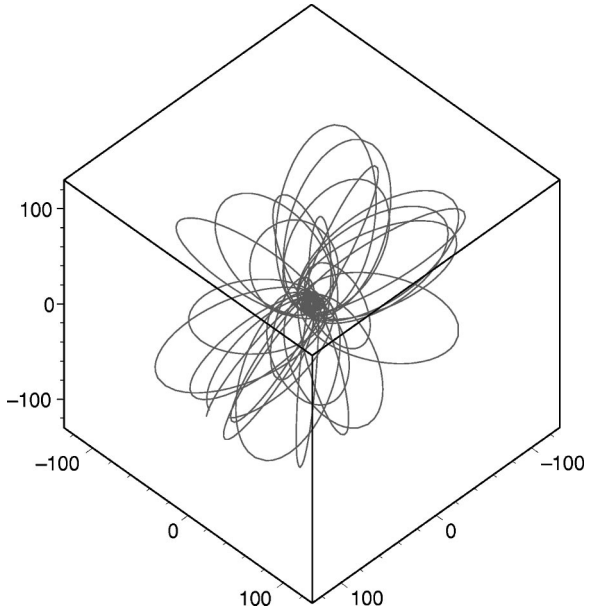

FIG. 2. Trajectory taken from the fractal basin boundary of Fig. 1. The axes are scaled in units of the total mass.

$-y$ plane with initial conditions $(\mathbf{x},\dot{\mathbf{x}})=(5.0M,0,0,0,0.45,0)$ and spin alignments θ_1 and θ_2 relative to the orbital angular momentum. The bodies have a 1:3 mass ratio and spins $S_i=0.6m_i^2$. The trajectories were color coded according to their outcomes: Black for merger from above the $x-y$ plane, dark gray for merger from below the $x-y$ plane, white for more than 50 orbits, and light gray for escape beyond $r=1000M$. The lower panel in Fig. 1 is a detail of the fractal basin boundary, and the location of a long-lived orbit that lies close to the basin boundary. A portion of this trajectory is drawn in Fig. 2. The orbit has average period $T_o=1687M$, mean eccentricity $e=0.922$ and mean semimajor axis $a=66.7M$. Integrating the radiation reaction force along the trajectory gives a decay rate of $\langle\dot{E}\rangle=-1.26\times10^{-6}$. In Fig. 3

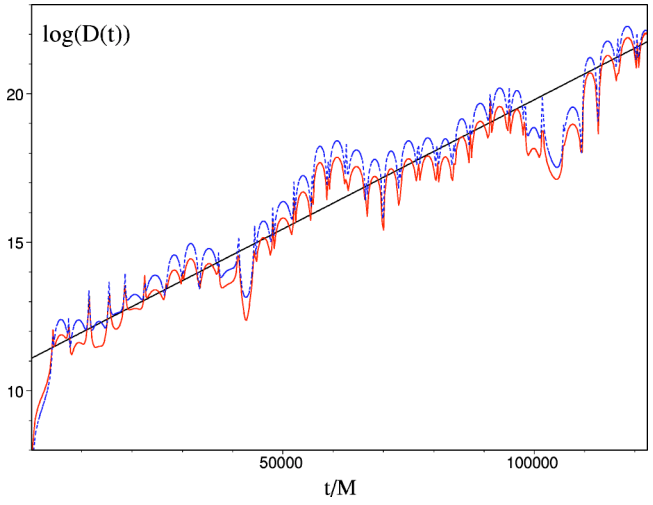

FIG. 3. Determining of the principal Lyapunov exponent for the trajectory in Fig. 2. The upper line uses method A, while the lower two lines (which lie over one another) use methods B and C.

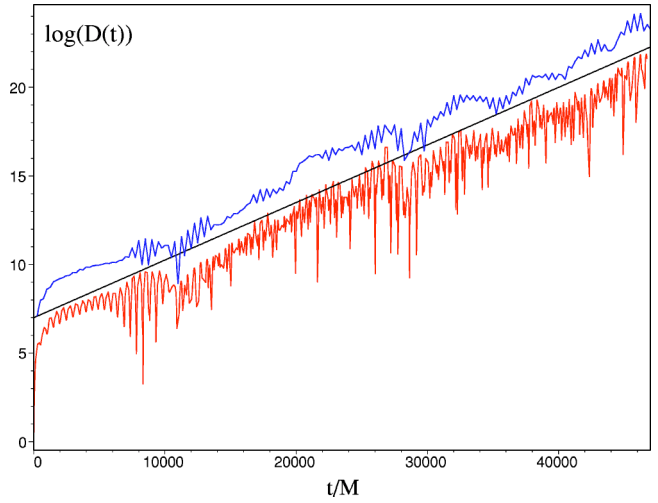

FIG. 4. Determination of the principal Lyapunov exponent for the less eccentric orbit described in the text. The upper line is $\log(d(t)/d(0))$ while the lower line is $\log(|\delta\Phi(t)|/|\delta\Phi(0)|)$.

we plot $\log(D(t)/D(0))$ for this trajectory using methods A, B and C described above. All three methods yield $T_\lambda=11500M\sim6.8T_o$ for the Lyapunov time scale, where we take an orbit to be a topological winding around the center of mass. The Lyapunov time scale is less than seven orbital periods, indicating that the motion is very chaotic.

Similar results were found for many other orbits taken from Fig. 1. Most of the orbits near the boundaries tend to be highly eccentric $(e>0.9)$, by virtue of being on the boundary and so on the cusp between merger and stability. It should be emphasized that high eccentricity is not required for chaotic behavior [4], although when both bodies spin there are *no* circular orbits whatsoever [9]. (In any case, highly eccentric orbits are important candidates for detection by the gravitational wave observatories [14].)

We did find some less eccentric orbits that had positive Lyapunov exponents. As an example of a less eccentric orbit, we show that the trajectory with initial conditions $(\mathbf{x},\dot{\mathbf{x}})=(5.5M,0,0,0,0.4,0)$, $\theta_1=\pi/2$, $\theta_2=\pi/6$, mass ratio 1:3 and spins $S_i=m_i^2$ is also highly chaotic. The orbit has average period $T_o=275M$, mean eccentricity $e=0.59$ and mean semimajor axis $a=13.7M$. Plots of $\log(D(t)/D(0))$ are drawn in Fig. 4. In this case we used method *C* and the phase divergence method to estimate T_λ. Both methods gave $T_\lambda=3080M=11.2T_o$, which indicates that the orbit is highly chaotic.

We found large numbers of orbits, with a range of mass ratios, spin parameters and spin alignments that had positive Lyapunov exponents. The time scale for the chaotic behavior was often a small multiple of the orbital period.

To further compare with Ref. [8], we took up their case of a binary with mass ratio 1:1 and spins $S_i=m_i^2$, $\theta_1=38^o$, $\theta_2=70^o$. We found a positive Lyapunov exponent for $(\mathbf{x},\dot{\mathbf{x}})=(5.0M,0,0,0,0.399,0)$. Therefore at least some of the equal mass binaries demonstrate chaotic orbits. As is common in chaotic systems, different trajectories came with different exponents, some of which were zero. For example, the orbit

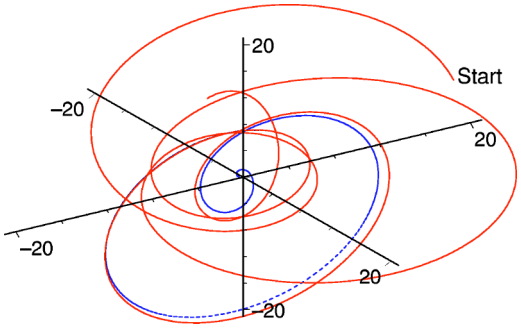

FIG. 5. A detail of trajectory (solid line) with the effect of radiation reaction (dotted line).

with initial conditions $(\mathbf{x},\dot{\mathbf{x}})=(5.0M,0,0,0,0.428,0)$ gave $\lambda_p=0$. Herein lies an inherent weakness of the Lyapunov exponents themselves. They vary from orbit to orbit. A much more powerful survey of the phase space scans for chaos using fractal basin boundaries as in Fig. 1.

We used four methods to determine λ_p, along with a battery of numerical tests, and our results have proven robust. We therefore confirm the chaos discovered in Refs. [2,4], contrary to the claims of Ref. [8]. It should also be emphasized that the fractal basin boundary method used in Ref. [2] is an unambiguous declaration of chaos, and alone stands as proof of chaotic dynamics [13,15]. Still, the Lyapunov time scales can be useful for determining the impact of chaos on the gravitational wave detection.

Now that we have confirmed that the 2PN dynamics is chaotic, we turn to the question of how significant the effect is. To this end we went to the next order in the post-Newtonian expansion and included the radiation reaction force. The effect of the radiation reaction force on the trajectory studied in Fig. 4 is shown in Fig. 5. Starting at an arbitrary point along the trajectory, we see that the radiation reaction force drives the evolution from inspiral to plunge in roughly 5 orbits. This is comparable to the Lyapunov time scale of roughly 11 orbits. It tells us that the chaotic behavior seen at 2PN order is marginal when radiation reaction is included. That is, chaos is damped by dissipation, but at least for some orbits the Lyapunov time scale is comparable to the dissipation time scale. Both the instability of the orbits and the degree of damping increase as merger is approached.

There is another way to show that the chaotic behavior found in the nondissipative 2PN dynamics does leave an imprint on the dissipative 2.5PN dynamics. The effect is illustrated in Fig. 6 where trajectories with initial conditions $(\mathbf{x},\dot{\mathbf{x}})=(30M,0,0,0,0.12,0)$, mass ratio 1:1 and spins $S_i=0.6m_i^2$ were evolved for a range of spin-orbit alignments. The initial conditions were color coded using the same scheme as before. Despite the damping, the outcomes are intertwined in a complicated fashion. As pointed out in Ref. [3], with dissipation the system will not have fully fractal boundaries. However, the imprint of the underlying chaos of the conservative system is recorded in the amount of structure in the basin boundaries before the fractal cuts off and is rendered smooth. The detailed view in the lower panel shows that the boundaries are eventually smooth rather than fractal.

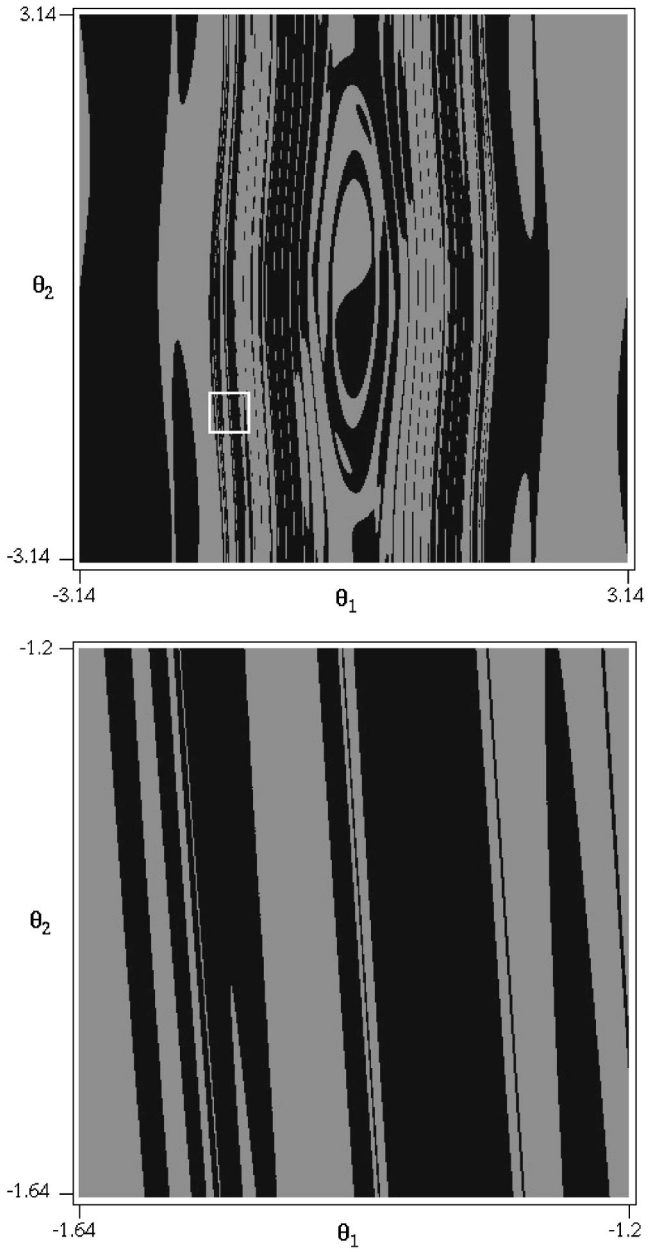

FIG. 6. Basin boundaries with radiation reaction. The upper panel shows a complicated intertwining of outcomes, however the detailed view reveals that the boundaries are not fractal.

It is worth comparing our results to the interesting work of Ref. [1]. The authors of Ref. [1] also found a positive Lyapunov exponent for spinning test particle motion around a Schwarzschild black hole. However, the light companion required an unphysically large spin many times maximal. Here we find that the additional nonlinearity from the gravitational interaction of the two bodies has introduced chaotic dynamics for physically realistic spins below maximal. We emphasize that the dynamics we study is only an approximation, but we think it is unlikely that the chaos is an artifact of the approximations. The very difficulty in solving the two-body problem in general relativity hints that the two-body problem itself, perhaps even without the addition of spins, is fully chaotic.

The effects that lead to the 2PN system being chaotic are most pronounced for the innermost orbits. Importantly, the very idea of locating the innermost stable circular orbit (ISCO) in the conserative system in order to mark the transition to merger must be abandoned. The underlying chaos of the conservative dynamics means that unstable periodic orbits crowd this region of phase space [17]. The fractal basin boundaries are a reflection of this fractal set of unstable periodic orbits. Consequently chaos may be significant for the final orbits and the transition to plunge, though techniques other than the post-Newtonian approximation are needed to study this transition [7].

In conclusion, there is chaos in the 2PN equations of motion for spinning compact binaries. The chaos is damped by dissipation at 2.5PN order so that most orbits will only be mildly influenced by the complicated dynamics.

N.J.C. is supported in part by National Science Foundation Grant No. PHY-0099532. J.L. is supported by PPARC and NESTA (National Endowment for Science Technology and Arts).

[1] S. Suzuki and K. Maeda, Phys. Rev. D **55**, 4848 (1997).
[2] J. Levin, Phys. Rev. Lett. **84**, 3515 (2000).
[3] N.J. Cornish, Phys. Rev. D **64**, 084011 (2001).
[4] J. Levin, Phys. Rev. D **67**, 044013 (2003).
[5] B.S. Sathyaprakash and B.F. Schutz, Class. Quantum Grav. **20**, S209 (2003).
[6] N.J. Cornish, Phys. Rev. Lett. **85**, 3980 (2000).
[7] S. Hughes, Phys. Rev. Lett. **85**, 5480 (2000).
[8] J.D. Schnittman and F.A. Rasio, Phys. Rev. Lett. **87**, 121101 (2001).
[9] L. Kidder, Phys. Rev. D **52**, 821 (1995).
[10] E. Poisson, Phys. Rev. D **57**, 5287 (1998).
[11] H. Tagoshi, A. Ohashi, and B. Owen, Phys. Rev. D **63**, 044006 (2001).
[12] P. Cvitanović, R. Artuso, R. Mainieri, G. Tanner, and G. Vattay, *Classical and Quantum Chaos*, www.nbi.dk/ChaosBook/, Niels Bohr Institute (Copenhagen 2001).
[13] C.P. Dettmann, N.E. Frankel, and N.J. Cornish, Phys. Rev. D **50**, R618 (1994).
[14] S.F. Portegies-Zwart and S.L. McMillan, astro-ph/9910061.
[15] N.J. Cornish and J.J. Levin, Phys. Rev. Lett. **78**, 998 (1997); Phys. Rev. D **55**, 7489 (1997).
[16] J. Levin, R. O'Reilly, and E.J. Copeland, Phys. Rev. D **62**, 024023 (2000).
[17] It is telling that the most unstable motion does appear to occur in the vicinity of the homoclinic orbits. Homoclinic orbits lie on the boundary between dynamical stability and instability [16]. The ISCO is a specific example of a homoclinic orbit.